Radionuclide imaging of cardiac autonomic innervation

Sang Yong Ji, MD,[a,b] and Mark I. Travin, MD, FASNC[a,b]

Cardiac autonomic function plays a crucial role in health and disease, with abnormalities both reflecting the severity of the disease and contributing specifically to clinical deterioration and poor prognosis. Radiotracer analogs of the sympathetic mediator norepinephrine have been investigated extensively, and are at the brink of potential widespread clinical use. The most widely studied SPECT tracer, I-123 metaiodobenzylguanidine (^{123}I-*m*IBG) has consistently shown a strong, independent ability to risk stratify patients with advanced congestive heart failure. Increased global cardiac uptake appears to have a high negative predictive value in terms of cardiac events, especially death and arrhythmias, and therefore and may have a role in guiding therapy, particularly by helping to better select patients unresponsive to conventional medical therapies who would benefit from device therapies such as an ICD (implantable cardioverter defibrillator), CRT (cardiac resynchronization therapy), LVAD (left ventricular assist device), or cardiac transplantation. Cardiac autonomic imaging with SPECT and PET tracers also shows potential to assess patients following cardiac transplant, those with primary arrhythmic condition, coronary artery disease, diabetes mellitus, and during cardiotoxic chemotherapy. Radiotracer imaging of cardiac autonomic function allows visualization and quantitative measurements of underlying molecular aspects of cardiac disease, and should therefore provide a perspective that other cardiac tests cannot.

Key Words: Sympathetic nervous system • radionuclide imaging • I-123 *m*IBG

INTRODUCTION

Autonomic neuronal innervation plays a critical role in cardiac function. The heart is richly innervated with sympathetic and parasympathetic fibers that work in conjunction with circulating catecholamine mediators, such as norepinephrine (NE), to precisely regulate cardiac output at rest and during periods of increased cardiovascular demand. An impairment of cardiac autonomic function, usually the result of cardiac disease, both reflects the severity of the condition and contributes to the pathophysiologic impairment that can worsen patient outcome. As cardiac autonomic function involves molecular processes, imaging with radionuclide tracers is an ideal method of assessment.

Cardiac autonomic function is controlled by various centers in the brain that respond to incoming signals from peripheral receptors. Sympathetic efferent signals following descending pathways from the brain through the spinal cord, synapsing with pre-ganglionic fibers that leave the spinal cord at levels T1-L3, subsequently synapsing with post-ganglionic fibers that innervate both ventricles. Sympathetic nerves follow the coronary arteries in the subepicardium before penetrating the myocardium. The principle chemical mediator of sympathetic function is norepinephrine.[1,2]

Parasympathetic fibers are scarce in comparison with sympathetic. They originate in the medulla and follow the vagus nerves. In the heart they start epicardially, cross the AV groove and then penetrate the myocardium, located thereafter in the subendocardium. Parasympathetic fibers innervate the atria but are scare in the ventricle (mostly the inferior wall), and also modulate SA and AV nodal function. The major chemical mediator of parasympathetic function is acetylcholine.

Most published literature and current clinical applicability of autonomic radionuclide imaging is of

From the Department of Nuclear Medicine,[a] and Division of Cardiology/Department of Medicine,[b] Montefiore Medical Center, Albert Einstein College of Medicine, Bronx, NY.

Reprint requests: Mark I. Travin, MD, FASNC, Department of Nuclear Medicine, Montefiore Medical Center, Albert Einstein College of Medicine, 111 East-210th Street, Bronx, NY 10467-2490; *mtravin@montefiore.org*.

J Nucl Cardiol 2010;17:655–66.
1071-3581/$34.00

doi:10.1007/s12350-010-9239-x

the sympathetic system, with parasympathetic imaging studies limited mostly to animals. Therefore, the following discussion will deal predominantly with cardiac sympathetic imaging.

RADIONUCLIDE TRACERS

Cardiac sympathetic innervation imaging currently focuses on the synaptic junction, illustrated in Figure 1.[3] Most radiotracers that have been developed image presynaptic anatomy and function, but newer tracers that bind to post-synaptic α and β receptors are also being designed and investigated.

Norepinephrine (NE) is produced in the presynaptic sympathetic nerve terminal through multiple biochemical processes starting with tyrosine, and ultimately stored at high concentrations in presynaptic vesicles. In response to a stimulus, the NE-containing vesicles are released into the synaptic space and bind to postsynaptic receptors, resulting in various cardiac stimulatory effects.[4,5]

Termination of the sympathetic response occurs through a transporter protein-mediated, sodium-, energy-, and temperature-dependent process, known as ''uptake-1,'' for storage and/or catabolic disposal. Some synaptic NE is also taken up by non-neuronal postsynaptic cells, probably by sodium-independent passive diffusion (i.e., the ''uptake-2'' system).[6,7]

Most neuronal imaging has been with radiolabeled analogs of norepinephrine. Guanethidine is a false neurotransmitter analog of NE that is taken up via the uptake-1 pathway. Chemical modification of guanethidine produces a molecule, metaiodobenzylguanidine

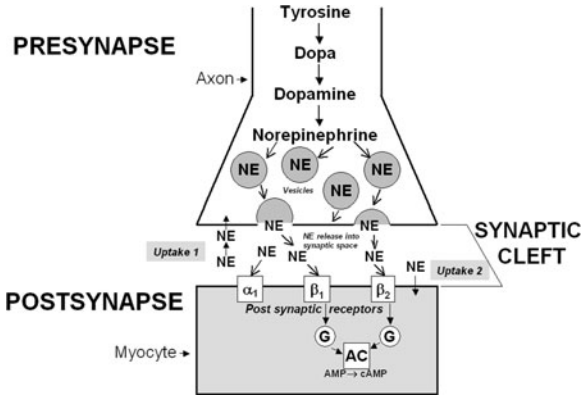

Figure 1. Schematic representation of sympathetic neuronal synapse. *AC*, adenyl cyclase; *AMP*, adenosine monophosphate; *cAMP*, cyclic adenosine monophosphate; *G*, G proteins; *NE*, norepinephrine. Reprinted from Cardiology Clinics: Nuclear Cardiology—From Perfusion to Tissue Biology, Vol. 27, Travin MI, Cardiac neuronal imaging at the edge of clinical application, p. 312, Copyright 2009, with permission from Elsevier.[3]

(*m*IBG) that can be labeled with radioactive iodine and therefore imaged. While early in its development *m*IBG was labeled with ^{131}I, the high energy emissions of this isotope and its relatively long half life of 8 days led to the development of the now preferred ^{123}I-*m*IBG. ^{123}I emits predominantly gamma photons with energies of 159 keV, and has a half-life of 13.2 hours, therefore well tolerated and easily imaged with a SPECT (single photon emission computed tomography) camera. Unlike NE, ^{123}I-*m*IBG is not catabolized by monoamine oxidase (MAO) or catechol-*o*-methyltransferase, allowing it to localize in myocardial sympathetic nerve endings to a higher cytoplasmic concentration than NE.[8-10] ^{123}I-*m*IBG has for many years been used for cardiac imaging in Europe and Japan, but in the US is at the time of this writing under FDA review for this purpose.

There are also various PET (positron emission tomography) analogs of norepinephrine under investigation.[6] Compared with ^{123}I-*m*IBG, current PET tracers are more similar to NE in composition, thereby having distinct biologic advantages, and they also have better physical properties for imaging. The most commonly investigated neuronal PET tracer is ^{11}C-meta-hydroxyephedrine (HED) that has higher uptake-1 selectivity than ^{123}I-*m*IBG, resulting in better differentiation between innervated and denervated myocardium, recently found to be of particular advantage in evaluating neuronal heterogeneity in hibernating myocardium.[11] In normal patients, ^{11}C-HED also appears to have more homogeneous uptake than ^{123}I-*m*IBG. Other less well-studied ^{11}C neuronal tracers include ^{11}C-epinephrine and ^{11}C-phenylephrine. The latter is rapidly metabolized by MAO and therefore could potentially play a role in assessment of vesicular storage function. More recently an ^{18}F labeled tracer has been developed and is under investigation.[12,13]

IMAGING METHODS AND INTERPRETATION

Intravenous injection of ^{123}I-*m*IBG is performed at rest, and needs only minimal preparation. Medications that might interfere with catecholamine uptake, such as various antidepressants, antipsychotics, and some calcium channel blockers, should be held for 24 hours before tracer injection and imaging. There are differences of opinion regarding the need for administration of thyroid-blocking agents before ^{123}I-*m*IBG administration. Historically such blockade has been undertaken to shield the thyroid from exposure to unbound impurities such as ^{124}I and ^{125}I, but with modern production methods the amount of impurities and unbound ^{123}I is minimal.

Tracer dosage has not been formally established. A dose of 3 to 5 mCi (111-185 MBq) over a 1-minute

period has been customarily used, and is generally satisfactory for planar image analysis. Nevertheless, as it is often difficult to obtain satisfactory SPECT images in patients who have severe cardiac dysfunction, a dose of up to 10 mCi (370 MBq) may be appropriate and is under consideration.[4]

Planar and SPECT images are routinely obtained approximately 15 minutes following tracer administration (early), and again 3 to 5 hours later (delayed). Although some believe that only the delayed image should be used for interpretation and analysis as it represents actual neuronal uptake (as opposed to interstitial uptake for the early images), tracer washout between early and delayed planar images may provide important additional information.[14,15]

Parameters for planar and SPECT acquisition of ^{123}I-*m*IBG are not formally established, but current methods are described in various published reviews.[1,16] Planar images are obtained in the anterior view for 10 minutes using an energy window of 159 keV ± 20%. SPECT images are obtained using the same energy window by way of a 180° circular acquisition from 45° right anterior oblique to 45° left posterior oblique, using a total of 60 stops (30 stops per head if done with a dual-headed camera) at 30 seconds per stop. Although low-energy collimators have customarily been used for ^{123}I-*m*IBG acquisition, multiple low-abundance higher-energy photon emissions (including one at 529 keV) are emitted by ^{123}I and more freely penetrate the septa, degrading image quality. Work is under way using a measured point spread function to perform three-dimensional deconvolution of the septal penetration to compensate for this effect and improve image accuracy, particularly for quantitative parameters that have different values when these corrections are applied.[17]

Interpretation of cardiac ^{123}I-*m*IBG images currently consists of assessment of global tracer uptake on planar images, tracer washout between early and delayed planar images, and regional uptake on tomographic images. The standard measure of global ^{123}I-*m*IBG uptake is the heart mediastinal ratio (HMR), derived through assessment of per pixel activity in a region of interest over the heart in reference to a background area in the upper mediastinum. The HMR has been derived in various ways in the literature and has not yet been standardized, although interestingly all methods appear to give similar results in any given patient study.[8,15,18,19] A recently reported normal value for HMR is 2.2 ± 0.3, with a ratio of <1.6 (2 standard deviations below the mean) considered to be abnormal and correlate with increased patient risk.[20]

^{123}I-*m*IBG washout (compensated for radioactive decay) may reflect turnover of catecholamines attributable to the sympathetic drive, and measures the ability of myocardium to retain *m*IBG. A normal value has been reported to be 10% ± 9%, with sicker patients having higher values.[15,21] Washout may correlate with increased sympathetic tone, but the complexity of this relationship has not been fully elucidated. Figure 2 shows examples of normal and abnormal planar cardiac ^{123}I-*m*IBG images.

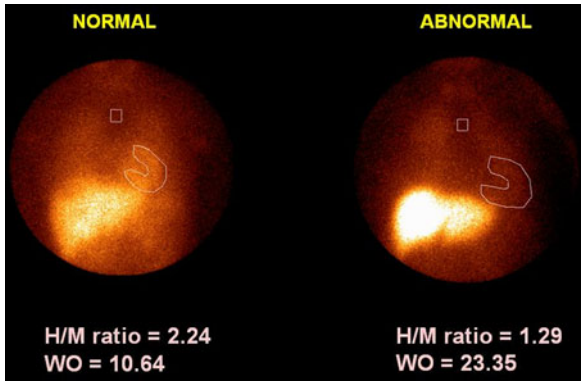

Figure 2. Examples of planar cardiac ^{123}I-*m*IBG images. The example on the left shows normal cardiac ^{123}I-*m*IBG uptake with a heart mediastinal (H/M) ratio of 2.24 and a normal tracer washout (WO) from initial to delayed images of 10.64%. The example on the right shows abnormal a heart mediastinal ratio of 1.29 in images with an abnormal tracer washout of 23.35%.

Assessing regional uptake of ^{123}I-*m*IBG on tomographic images is less well studied and established. The potential clinical utility is based on the concept that regional abnormalities may create areas of electrical instability predisposing to dangerous ventricular arrhythmias, particularly if these territories are perfused and have viable myocytes, i.e., a neuronal/perfusion mismatch that may produce denervation supersensitivity.[22-24] Difficulties with tomographic imaging include poor image quality in patients with markedly decreased cardiac uptake, overlying non-cardiac activity (lung and liver) interfering with image reconstruction, and a frequently reported heterogeneity of regional ^{123}I-*m*IBG uptake in normal patients that may vary with age and gender.[21,25,26] There are reports of less normal variation when PET tracers such as ^{11}C-HED are used that may be related both to differences in soft tissue attenuation and in tracer properties and kinetics.[27]

NEURONAL IMAGING IN CONGESTIVE HEART FAILURE

Congestive heart failure (CHF) is a worsening epidemic in developed countries due in large part to a progressively aging population and to better survival

from acute cardiac events that leave patients with damaged hearts. In the United States close to 5 million people have CHF, with 550,000 new cases each year. Mortality can reach 50% annually, with CHF being a major underlying or contributing cause of death in close to 300,000 people per year. CHF is an expensive condition with more Medicare dollars spent on it than on any other condition, promising to go even higher with the increasing use of devices.[28,29]

Despite dramatic improvements in diagnosis and treatment of CHF, there remain major knowledge gaps in the prediction of treatment response and disease progression, making imperative the need for better understanding of the biomolecular pathophysiology and its translation into clinical outcomes.[30] As CHF is in large part a condition involving disruption of the neurohormonal state, cardiac neuronal innervation is thought to play a crucial role. An increased sympathetic response is initially favorable by serving as compensation for decreased cardiac output, but as CHF progresses this response leads to deleterious neurohormonal and myocardial structural changes that worsen the condition and increase the likelihood of arrhythmias and cardiac death. Numerous studies have shown that assessment of the cardiac autonomic state with radiotracers such as ^{123}I-*m*IBG can evaluate the cardiac condition beyond that available from conventional markers, can help track the effects of therapeutic interventions, and could potentially help guide therapy in a cost-effective manner. Among ^{123}I-*m*IBG image changes observed in CHF is increased washout, perhaps the result of competition for the uptake-1 process by increased circulating NE, and decreased HMR as CHF becomes more advanced with loss of sympathetic neurons and/or impaired uptake-1 function.[31]

Studies have consistently shown that a decreased ^{123}I-*m*IBG HMR predicts a poor prognosis in patients with advanced CHF.[32-34] Among the first to demonstrate this was Merlet et al in a study of 90 patients with severe CHF and mean left ventricular ejection fraction (LVEF) of 22%. Patients with HMR < 1.2 had a 12-month survival of 40% compared with 100% for patients with a higher ratio. Multivariate analysis showed that HMR was a better predictor of outcome than LVEF and heart size.[35] Nakata et al showed that prognosis progressively worsened in CHF patients as the HMR got lower,[36] and Wakabayashi et al demonstrated that HMR predicted outcome for CHF of both ischemic and non-ischemic origin.[37]

Similarly, increased ^{123}I-*m*IBG washout worsens prognosis in patients with CHF. Ogita et al showed that in patients with CHF and LVEF $< 40\%$, over a 4-year period those with tracer washout $\geq 27\%$ had a 35% cardiac death rate compared with 0 deaths in patients with normal washout.[15] There was also a greater than threefold increase in hospital admissions for CHF in the high washout group. A later study from the same group reported that increased washout predicts sudden cardiac death.[38]

More recently, larger, carefully designed multicenter studies have been undertaken to examine the potential role of ^{123}I-*m*IBG imaging in CHF. Agostini and colleagues reported on 290 CHF involving six sites in Europe, finding that by logistic regression the only significant predictors of major cardiac events—cardiac death, need for transplant, and potentially fatal arrhythmias—over 2 years was LVEF and HMR.[39] Particularly striking was the ability of HMR to risk stratify patients who had LVEF $\leq 35\%$, with event rates ranging from less than 5% for those who had HMR ≥ 2.18, to more than 50% for those who had HMR ≤ 1.45. At the same time, patients with a higher LVEF of 35-49% who had HMR ≤ 1.45 had an event rate $>10\%$.

Most recently the ADMIRE-HF (AdreView Myocardial Imaging for Risk Evaluation in Heart Failure, AdreView = ^{123}I-*m*IBG) study was undertaken in 96 sites in the US, Canada, and Europe, in which 961 patients with NYHA (New York Heart Association) Class II-III CHF and LVEF $\leq 35\%$ underwent rest and delayed ^{123}I-*m*IBG imaging.[20] The primary goal was to relate an HMR < 1.6 on the 4-hour delayed planar image with the occurrence of progression of CHF (worsening NYHA Class), a potentially life threatening arrhythmia, and/or cardiac death over a 2-year follow-up. As shown in Figure 3, the HMR well separated patients with and without cardiac events. However, approximately 2/3 of these events were CHF progression. When data analysis focused on the 201

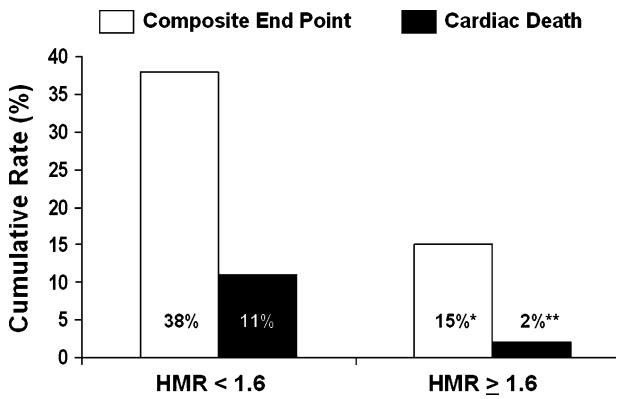

Figure 3. Cumulative 2-year event rates comparing subjects with HMR < 1.6 vs ≥ 1.6. Composite end point includes heart failure progression, arrhythmic events, and cardiac mortality. $*P < .0001$ compared with HMR < 1.6; $**P < .001$ compared with HMR < 1.6. *HMR*, Heart mediastinal ratio.[40]

(21%) of patients with HMR ≥ 1.6, there were only two cardiac deaths, indicating that in such patients with advanced CHF a normal HMR predicted a <1% yearly risk of cardiac death.[40] A subsequent multivariate analysis substudy showed that HMR was a predictor of both cardiac and all-cause death independent of other clinical and image variables, including age, LVEF, and BNP (brain natriuretic peptide).[41]

POTENTIAL ROLE OF ^{123}I-*MIBG IN GUIDING THERAPY FOR CHF

While the use of cardiac adrenergic imaging to risk stratify patients may have value in itself, the potential to more effectively guide specific therapies would provide greater clinical utility. There are numerous reports demonstrating that ^{123}I-*m*IBG imaging effectively monitors the effects of conventional CHF medical therapies. As one might expect, ^{123}I-*m*IBG images frequently improve after institution of β-blocker therapy, associated in some studies with decreased ventricular volumes, improved LVEF, and symptom relief.[18,42-45] Nevertheless, various other medications that do not directly influence cardiac sympathetic function, i.e., ACE (angiotensin converting enzyme) inhibitors, ARB (angiotensin receptor blocking) agents, spironolactone, and amiodarone also lead to improvements in ^{123}I-*m*IBG image findings.[46-50] It is important to consider how the above findings could specifically direct therapy. Use of ^{123}I-*m*IBG to decide who might benefit from a particular medical therapy such as β-blockers has shown insufficient separation,[51,52] and given the high benefit to risk/cost ratio of conventional medical therapies, a cardiac ^{123}I-*m*IBG study is unlikely to preclude their use.[53] ^{123}I-*m*IBG imaging might instead be more useful as an indicator of whether or not a patient's medical therapy is working satisfactorily, and could therefore help determine whether higher risk and usually more expensive device therapies or cardiac transplantation are needed.[32] A study by Matsui et al of patients with severe cardiomyopathy showed that a worsening HMR after 6 months of optimal medical therapy had, with BNP, the highest, independent predictive value for cardiac death.[54] It is possible that in patients with worsening HMR on serial studies, institution of additional or alternate therapies, such as devices, need to be undertaken to improve outcome. A recent study by Drakos et al of patients on LVAD (left ventricular assist device) therapy found that clinical improvement paralleled improvement in ^{123}I-*m*IBG image parameters.[55] Alternatively, a recent study showed that a decreased HMR was associated with poor response to cardiac resynchronization therapy.[56]

^{123}I-*MIBG IMAGING AND VENTRICULAR ARRHYTHMIAS

A major cause of death in patients with advanced heart failure is ventricular arrhythmia-induced sudden cardiac death (SCD).[57] While in some cases the terminal arrhythmia is the natural result of end-stage irreversible pump dysfunction, in other cases a patient may otherwise be doing relatively well only to be struck down by SCD. For the latter reason, based on trials such as SCD-HEFT, it is a Class IA indication that patients with LVEF ≤ 35% receive a prophylactic implantable cardioverter defibrillator (ICD) for primary prevention.[58,59] Nevertheless, most patients who receive an ICD based on these criteria do not use their device,[60-62] with it widely acknowledged that LVEF is an imperfect measure of the risk of arrhythmic death.[63-65] Given the potentially adverse clinical consequences of ICD implantation, including operative complications, device malfunction, pain, psychiatric problems associated with shocks, and life style restrictions, as well as a cost of about $28,000 for the device, a better approach for deciding who should get an ICD is needed.[66]

Although mechanisms of cardiac arrhythmias are complex and multifactorial, the cardiac autonomic nervous system is a crucial component,[5,67] suggesting a potential role of ^{123}I-*m*IBG imaging to help better identify at risk patients who would benefit from an ICD. Early dog studies showed that artificial creation of focal areas of cardiac denervation resulted in regional ^{123}I-*m*IBG defects associated with production of supersensitive action potential refractory periods.[24] Other work has shown an association between focal ^{123}I-*m*IBG defects and ventricular arrhythmias on Holter monitoring.[68,69]

As performing clinical research studies on SCD is difficult, particularly given that ascertaining a definitive arrhythmic cause of death is often not possible, a suitable group to investigate would be patients who already have an ICD. Although occurrence of an ICD shock in these patients does not necessarily mean that they would have experienced SCD if not for the device, it may be one suitable method to use at this time. With this approach, Arora and colleagues performed a pilot study on 17 patients with advanced CHF who already had an ICD, deliberately selecting a balanced group of patients with and without prior ICD discharges.[70] A reduced late HMR (threshold 1.54) was associated with increased likelihood of an ICD discharge, with a positive predictive value of 71% and a negative predictive value of 17%. Combining autonomic imaging with heart rate variability (HRV) analysis, none of three patients who had both a high HMR and a more abnormal HRV had an ICD discharge, whereas all four patients who had a low

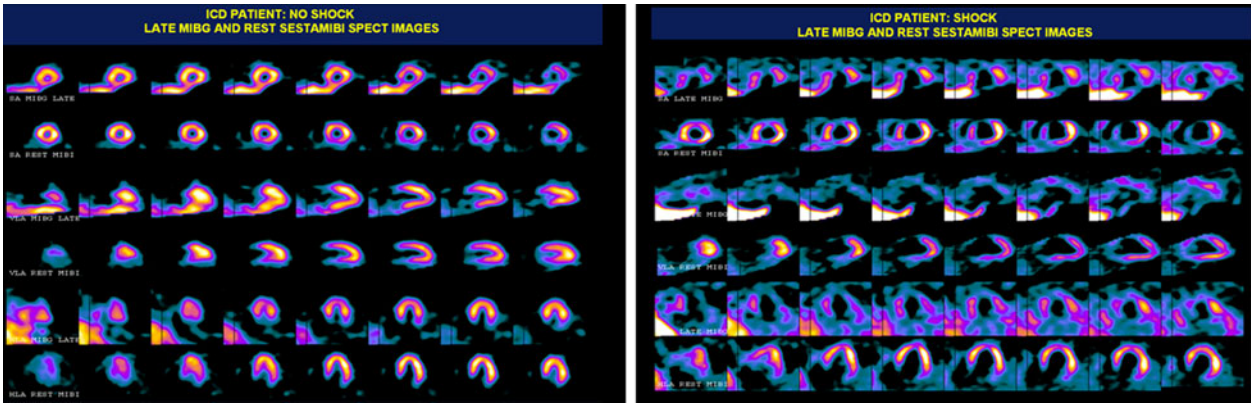

Figure 4. ^{123}I-*m*IBG (neuronal) and ^{99m}Tc-sestamibi (perfusion) SPECT images in patients with ICDs. The images on the left are from a patient without an ICD shock, and show both homogeneous neuronal and perfusion tracer uptake. The images on the right are from a patient who had received numerous appropriate ICD shocks, and show neuronal/perfusion mismatching defects involving the inferior, inferolateral, and apical walls; there is a matched defect in the anterior wall. *HLA*, horizontal long axis; *ICD*, implantable cardioverter defibrillator; *MIBG*, metaiodobenzylguanidine (^{123}I-*m*IBG); *MIBI*, ^{99m}Tc-sestamibi; *SA*, short axis.

HMR and less abnormal HRV did. In addition, patients who had ICD discharges had more extensive ^{123}I-*m*IBG/perfusion (^{99m}Tc-sestamibi) mismatches on SPECT imaging. All patients in this study also had tomographic ^{123}I-*m*IBG and perfusion (^{99m}Tc-sestamibi) imaging. Those with autonomic perfusion mismatches were more likely to have appropriate ICD discharges than those without, with case examples seen in Figure 4.

A subsequent study by Nagahara and colleagues showed that SCD or an appropriate ICD discharge strongly correlated with late HMR independent of numerous other variables, including LVEF.[71] Combining HMR with LVEF or BNP gave additional predictive power. Finally, Kioka and colleagues reported an association of high ^{123}I-*m*IBG washout and SCD.[38]

In ADMIRE-HF combined ''arrhythmic'' events (self-limited ventricular tachycardia, resuscitated cardiac arrest, appropriate ICD discharges) were more common in subjects with HMR < 1.60 (10.4%) than in those with HMR ≥ 1.6 (3.5% $P < 0.01$).[40] As illustrated in Figure 5 from a subanalysis by Senior et al, the highest arrhythmic rate was in patients with an intermediate decrease in HMR, while patients with an extremely low HMR were less often had an arrhythmic event, but rather were more likely to die from pump failure.[72] Also of interest in this subanalysis, of patients without an ICD who had HMR ≥ 1.6, there was only one arrhythmic death. In another recent study, Boogers et al performed ^{123}I-*m*IBG SPECT imaging in patients prior to ICD implantation, finding that over a mean 23-month follow-up (up to 3 years), the late tomographic

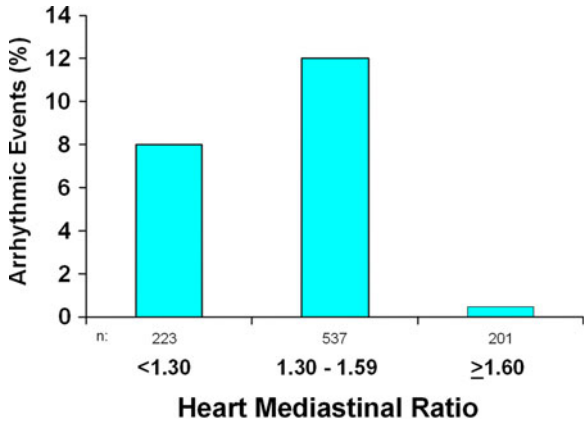

Figure 5. Arrhythmic events vs heart mediastinal ratio.[72]

defect score was an independent predictor of appropriate ICD therapy and cardiac death.[73]

In summary, recent large studies consistently show that cardiac neuronal imaging provides better predictive potential for SCD in CHF patients than currently accepted standards of LVEF and NYHA class, and in at least one study better than various ECG criteria.[74] Of course, further validation is merited before wider acceptance and consideration of ^{123}I-*m*IBG imaging in CHF and arrhythmia consensus guidelines. A high negative predictive value is crucial. At the same time, cardiac neuronal imaging could potentially identify those patients with CHF in the ''lower risk'' subgroups (e.g., LVEF $\geq 35\%$) who are in fact at significant risk of SCD that may indicate an ICD.

PRIMARY ARRHYTHMIC DISEASE

In addition to having potential clinical utility in CHF-associated ventricular arrhythmias, imaging with ^{123}I-*m*IBG or similar tracers has shown cardiac abnormalities in patients with primary arrhythmic conditions. Mitrani and colleagues saw regional sympathetic denervation in 55% of patients who presented with VT but had structurally normal hearts compared with none in controls.[75] Gill and colleagues found asymmetrical uptake of ^{123}I-*m*IBG in about half of the patients they studied who had VT and ''clinically normal'' hearts, particularly obvious in patients who had exercise-induced VT.[76]

Neuronal tracer uptake abnormalities are also seen in some of the more specifically characterized primary arrhythmic disorders. Schäfers and colleagues found abnormal ^{11}C-HED uptake distribution in patients with idiopathic right ventricular outflow tract tachycardia, as well as decreased uptake of the postsynaptic tracer ^{11}C-CGP12177 indicating reduced density of postsynaptic β-adrenoceptor density.[77] Neuronal tracer uptake in Brugada syndrome is especially interesting in that ^{123}I-*m*IBG defects seem localized to the inferior and inferoseptal walls, suggesting that a local dominance of parasympathetic tone in these regions may be related to a propensity for arrhythmogenesis.[78]

CARDIAC TRANSPLANTATION

During cardiac transplantation, postganglionic sympathetic fibers of the donor heart are interrupted, resulting in complete sympathetic denervation of the transplanted heart. The new heart thus has an impaired response to the demands of exercise. Over time, though, at least some sympathetic reinnervation occurs.[79-81] Bengel and colleagues used ^{11}C-HED imaging to demonstrate progressive post-transplant cardiac reinnervation, with a follow-up study showing a correlation with an enhanced contractile response to exercise and improved exercise times.[82,83] On the other hand, the absence of reinnervation could indicate complications and co-morbidities such as a coronary vasculopathy.

^{123}I-*M*IBG IMAGING IN ISCHEMIC HEART DISEASE

Sympathetic nerve trunks course along the coronary arterial pathways before penetrating the myocardium. Myocardial ischemia/infarction disrupts sympathetic transmission, in which case myocardium distal to and beyond the site of injury but not otherwise involved in the ischemic process may be affected. In addition cardiac sympathetic nervous tissue is more sensitive to ischemia than myocytes, and takes longer to recover. The result can be perfused and viable, but denervated myocardium, with such areas exhibiting denervation supersensitivity that predisposes to arrhythmias. Simões et al found that the presence of post MI ^{123}I-*m*IBG/^{201}Tl imaging mismatches correlated with electrophysiological abnormalities of prolonged QTc intervals and delayed depolarization on signal averaged ECG, both considered to predispose to lethal arrhythmias, although there were insufficient cardiac events to assess prognostic implications.[22] Sasano et al, using a pig model to create LAD infarcts, found that the creation of perfusion/innervation mismatches increased inducibility of sustained VT.[23] In accordance with the above discussion of CHF, ^{123}I-*m*IBG and other methods of neuronal imaging could also potentially guide post-MI ICD patient selection.

Another potential use of ^{123}I-*m*IBG imaging in ischemic heart disease takes advantage of the persistence of neuronal injury after resolution of the ischemic insult, i.e., ischemic memory. Watanabe and colleagues performed rest ^{123}I-*m*IBG studies on patients within 2 weeks of documented vasospastic angina on cardiac catheterization, and found that tracer defects were seen in 100% of the ^{123}I-*m*IBG images despite no Tl-201 perfusion abnormalities appreciated, versus in only 86% of ^{123}I-BMIPP (β-Methyl-*p*-[^{123}I]-iodophenyl-pentadecanoic acid) images.[84] Similarly, in a study by Tomoda et al, 24 ± 12 days after an ischemic attack, only 4 of 8 patients with non-Q-wave MI had a Tl-201 perfusion defect whereas all 8 had an ^{123}I-*m*IBG defect. In the same study, none of 12 patients with unstable angina had a Tl-201 defect, 7 of 12 had an ^{123}I-*m*IBG defect.[85]

^{123}I-*M*IBG IMAGING AND DIABETES MELLITUS

Diabetes is a systemic, multi-organ disease, with morbidity and mortality increased by the presence of autonomic neuropathy. While various noninvasive tests help to detect the presence of diabetic-induced neuropathy, they predominantly assess parasympathetic function. Cardiac imaging assessment of sympathetic function may provide a unique approach to assess neuropathy. Stevens and colleagues found abnormalities of ^{11}C-HED retention in 40% of autonomic neuropathy-free diabetic patients, first appearing in the inferior wall and then spreading to other parts of the heart. In patients who had severe neuropathies, increased absolute tracer retention (hyperinnervation) was seen in proximal myocardial segments in combination with more decreased retention (denervation) in distal segments, an innervation pattern that could result in electrical instability and predispose to life-threatening arrhythmias.[86]

The promise of using autonomic imaging to identify higher risk patients with DM was supported in a study by Nagamachi of type II patients who had no evidence of organic heart disease, followed a mean of 7.2 years. By multivariate analysis, a combination of decreased HMR on a delayed ^{123}I-*m*IBG image and an abnormality on HRV predicted cardiac events, whereas abnormal delayed HMR alone was an independent predictor of all-cause mortality.[87]

Further work is needed to determine the value and practicality of neuronal imaging in diabetics, especially those without evidence of end organ damage. Neuronal imaging may identify patients who have subclinical ischemic coronary disease and need more aggressive management, and may find patients with autonomic heterogeneities predisposing to lethal arrhythmias.

^{123}I-*M*IBG IMAGING AND CHEMOTHERAPY

Given the enhanced sensitivity of sympathetic nerves to myocardial insults, neuronal imaging has been investigated as a potential method of assessing cardiac damage from chemotherapy. In rat studies, Wakasugi and colleagues showed that doxorubicin administration resulted in a decrease in cardiac uptake of ^{125}I-*m*IBG, preceding a decrease in LVEF.[88] In humans, Olmos and colleagues reported decreased cardiac uptake of ^{123}I-*m*IBG as the cumulative dose of doxorubicin increased, followed by subsequent deterioration in LVEF.[89] Carrió and colleagues showed that at a cumulative doxorubicin dose of 240-300 mg · m^2 there was a correlation of cardiac ^{123}I-*m*IBG abnormalities with cardiac uptake of ^{111}In antimyosin antibody, but there was no clear association between decreased ^{123}I-*m*IBG uptake and severe LV functional impairment.[90] The potential role of ^{123}I-*m*IBG imaging in patients with chemotherapy shows promise, but still needs further investigation, particularly determining how it would add to currently used monitoring techniques.

POSTSYNAPTIC SYMPATHETIC IMAGING

Cardiac postsynaptic receptors transmit sympathetic signal to the myocardial tissue, regulating chronotropic, dromotropic, and inotropic cardiac effects, and are good targets for imaging. At this time only a few radiotracers have been synthesized for it, the main problem being the difficulty of finding a compound that is easily made and has sufficient specificity.[91] Some clinical work has been done with ^{11}CCGP12177, a nonselective, hydrophilic β-receptor binding agent that produces good-quality cardiac PET images. Caldwell and colleagues studied 13 patients with ischemic CHF and 25 age-matched healthy controls using ^{11}C-HED for presynaptic imaging and ^{11}C-CGP12177 to assess postsynaptic β-adrenergic receptor (BAR) density.[92] Although patients with CHF had a decrease in ^{11}C-HED and in BAR density compared with controls, the decrease in HED uptake was significantly greater, resulting in marked presynaptic/postsynaptic mismatch, especially in the inferior and lateral walls. Of four patients who had an adverse event over 18 months, three had a mean mismatch score greater than six standard deviations above the mean of healthy subjects.

IMAGING OF THE CARDIAC PARASYMPATHETIC SYSTEM

Abnormalities of parasympathetic activity also contribute to cardiac pathophysiology. Parasympathetic innervation and activation can induce and maintain atrial fibrillation, whereas ablation can induce parasympathetic denervation and improve clinical outcome.[93,94] Due to the lack of sufficient experience and data, imaging of cardiac parasympathetic system has been limited. There is a low density of cholinergic neurons in the heart, as well as difficulty in tracer design because of rapid degradation of acetylcholine by esterase and a high specificity of the presynaptic receptor system for acetylcholine. Vesamicol is the base structure for tracer design. ^{18}F-FEOBV and has been investigated in rats, but it has a low myocardial specificity. ^{11}C-MQNB is a postsynaptic muscarinic receptor agonist, with some work done in humans. ^{18}F-D-Glucose-A85380 visualizes nicotinic acetylcholine receptors and has been used in humans with neurodegenerative disorders.[91]

CONCLUSIONS

Disruption of the cardiac neuronal system may occur as a result of cardiac disease and/or itself may be the cause of cardiac problems. Cardiac neuronal abnormalities occur in a variety of cardiac disease states and patients with cardiac neuronal abnormalities are at increased risk, including a higher potential for sudden, arrhythmic death. Thus, the ability to image cardiac neuronal system with radiotracers should be a powerful tool to assess and risk-stratify patients, and to guide the therapeutic approach in terms of pharmacologic therapy, implantation of mechanical devices, and determining the need for further intervention such as cardiac transplantation. Given that radiotracer imaging allows visualization and quantitative measurements of the underlying molecular aspects of cardiac disease, it should provide a perspective that other cardiac tests cannot.

References

1. Carrió I. Cardiac neurotransmission imaging. J Nucl Med 2001;42:1062-76.
2. Zipes DP. Autonomic modulation of cardiac arrhythmias. In: Zipes DP, Jalife J, editors. Cardiac electrophysiology: From cell to bedside. 2nd ed. Philadelphia: W.B. Saunders Company; 1995. p. 441-2.
3. Travin MI. Cardiac neuronal imaging at the edge of clinical application. Cardiol Clin 2009;27:311-27.
4. Flotats A, Carrió I. Cardiac neurotransmission SPECT imaging. J Nucl Cardiol 2004;11:587-602.
5. Verrier RL, Antzelevich C. Autonomic aspects of arrhythmogenesis: The enduring and the new. Curr Opin Cardiol 2004;19:2-11.
6. Bengel FM, Schwaiger M. Assessment of cardiac sympathetic neuronal function using PET imaging. J Nucl Cardiol 2004;11: 603-16.
7. Sisson JC, Wieland DM. Radiolabelled meta-iodobenzylguanidine pharmacology: Pharmacology and clinical studies. Am J Physiol Imaging 1986;1:96-103.
8. Hattori N, Schwaiger M. Metaiodobenzylguanidine scintigraphy of the heart. What have we learned clinically? Eur J Nucl Med 2000;27:1-6.
9. Kline RC, Swanson DP, Wieland DM, Thrall JH, Gross MD, Pitt B, Beierwaltes WH. Myocardial imaging in man with I-123 Metaiodobenzylguanidine. J Nucl Med 1981;22:129-32.
10. Wieland DM, Brown LE, Rogers WL, et al. Myocardial imaging with a radioiodinated norepinephrine storage analog. J Nucl Med 1981;22:22-31.
11. Luisi AJ, Suzuki G, deKemp R, et al. Regional ^{11}C-hydroxyephedrine retention in hibernating myocardium: Chronic inhomogeneity of sympathetic innervation in the absence of infarction. J Nucl Med 2005;46:1368-74.
12. Bozek J, Silva P, Lamoy M, Azure M, Radeke H, Robinson S, Yu M. Heart failure imaging in the rat with LMI1195: A new PET cardiac neuronal imaging agent. Circulation 2009;120:S362.
13. Yu M, Guaraldi M, Bozek J, Lamoy M, Silva P, Kagan M, Onthank D, Mistry M, Lazewatsky J, Broekema M, Radeke H, Puorhit A, Azure M, Cesati R, Casebier D, Robinson S. LMI1195: A new 18F benzylguanidine analog for PET cardiac sympathetic neuronal imaging. J Am Coll Cardiol 2010;55:A88.
14. Somsen GA, Verberne HJ, Fleury E, Righetti A. Normal values and within-subject variability of cardiac I-123 MIBG scintigraphy in healthy individuals: Implications for clinical studies. J Nucl Cardiol 2004;11:126-33.
15. Ogita H, Shimonagata T, Fukunami M, et al. Prognostic significance of cardiac ^{123}I metaiodobenzylguanidine imaging for mortality and morbidity in patients with chronic heart failure: A prospective study. Heart 2001;86:656-60.
16. Patel AD, Iskandrian AE. MIBG imaging. J Nucl Cardiol 2002;9:75-94.
17. Chen JI, Garcia EV, Galt JR, Folks RD, Carrió I. Optimized acquisition and processing protocols for I-123 cardiac SPECT imaging. J Nucl Cardiol 2006;13:251-60.
18. Agostini D, Belin A, Amar MH, et al. Improvement of cardiac neuronal function after carvedilol treatment in dilated cardiomyopathy: A ^{123}I-MIBG scintigraphic study. J Nucl Med 2000;41: 845-51.
19. Yamada T, Shimonagata T, Fukunami M, et al. Comparison of the prognostic value of cardiac iodine-123 metaiodobenzylguanidine imaging and heart rate variability in patients with chronic heart failure. J Am Coll Cardiol 2003;41:231-8.
20. Jacobson AF, Lombard J, Banerjee G, Camici PG. ^{123}I-*m*IBG scintigraphy to predict risk for adverse cardiac outcomes in heart failure patients: Design of two prospective multicenter international trials ADMIRE-HF study. J Nucl Cardiol 2009;16:113-21.
21. Morozumi T, Kusuoka H, Fukuchi K, Tani A, Uehara T, Matsuda S, Tsujimura E, Ito Y, Hori M, Kamada T, Nishimura T. Myocardial iodine-123-metaiodobenzylguanidine images and autonomic nerve activity in normal subjects. J Nucl Med 1997;38: 49-52.
22. Simões MV, Barthel P, Matsunari I, Nekolla SG, Schömig A, Schwaiger M, Schmidt G, Bengel FM. Presence of sympathetically denervated but viable myocardium and its electrophysiologic correlates after early revascularised, acute myocardial infarction. Eur Heart J 2004;25:551-7.
23. Sasano T, Abraham R, Chang KC, Ashikaga H, Mills KJ, Holt DP, Hilton J, Nekolla SG, Dong J, Lardo AC, Halperin H, Dannals RF, Marbán E, Bengel FM. Abnormal sympathetic innervation of viable myocardium and the substrate of ventricular tachycardia after myocardial infarction. J Am Coll Cardiol 2008;51:2266-75.
24. Minardo JD, Tuli MM, Mock BH, Weiner RE, Pride HP, Wellmann HN, Zipes DP. Scintigraphic and electrophysiologic evidence of canine myocardial sympathetic denervation and reinnervation produced by myocardial infarction or phenol application. Circulation 1988;78:1008-19.
25. Gill JS, Hunter GJ, Gane G, Camm AJ. Heterogeneity of the human myocardial sympathetic innervation: In vivo demonstration by iodine 123-labeled meta-iodobenzylguanidine scintigraphy. Am Heart J 1993;126:390-8.
26. Tsuchimochi S, Tamaki N, Tadamura E, Kawamoto M, Fujita T, Yonekura Y, Konishi J. Age and gender differences in normal myocardial adrenergic neuronal function evaluated by iodine-123-MIBG imaging. J Nucl Med 1995;36:969-74.
27. Hubertus Bülow H, Nekolla SG, Schwaiger M, Bengel F. Comparison of the normal distribution of three tracers used for evaluation of the presynaptic sympathetic neuron. J Nucl Cardiol 2003;10:S44.
28. Lim ET, Lahiri A. Should we be screening for myocardial hibernation in heart failure? J Nucl Cardiol 2004;11:114-7.
29. Hunt SA, Abraham WT, Chin MH, Feldman AM, Francis GS, Ganiats TG, Jessup M, Konstam MA, Mancini DM, Michi K, Oates JA, Rahko PS, Silver MA, Stevenson LW, Yancy CW. ACC/AHA 2005 guidelines update for the diagnosis and management of chronic heart failure in the adult: Summary article: A report of the American College of Cardiology/American Heart Association Task Force on Practice Guideline (Writing Committee to Update the 2001 Guidelines for the Evaluation and Management of Heart Failure). J Am Coll Cardiol 2005;46: 1116-43.
30. Tang WH, Francis GS. The year in heart failure. J Am Coll Cardiol 2005;46:2125-33.
31. Chen GP, Tabibiazar R, Branch KR, Link JM, Caldwell JH. Cardiac receptor physiology and imaging: An update. J Nucl Cardiol 2005;12:714-30.
32. Merlet P, Benvenuti C, Moyse D, Pouillart F, Dubois-Randé J, Duval A, Loisance D, Castaigne A, Syrota A. Prognostic value of MIBG imaging in idiopathic dilated cardiomyopathy. J Nucl Med 1999;40:917-23.
33. Anastasiou-Nana MI, Terrovitis JV, Athanasoulis T, Karaloizos L, Geramoutsos A, Pappa L, Tsagalou EP, Efentakis S, Nanas JN. Prognostic value of iodine-123-metaiodobenzylguanidine myocardial uptake and heart rate variability in chronic congestive heart failure secondary to ischemic or idiopathic dilated cardiomyopathy. Am J Cardiol 2005;96:427-31.
34. Arimoto T, Takeishi Y, Niizeki T, Nozaki N, Hirono O, Watanabe T, Nitobe J, Tsunoda Y, Suzuki S, Koyama Y, Kitahara T, Okada A, Takahashi K, Kubota I. Cardiac sympathetic denervation and

ongoing myocardial damage for prognosis in early stages of heart failure. J Cardiac Fail 2007;13:34-41.
35. Merlet P, Valette H, Dubois-Randé J, Moyse D, Duboc D, Dove P, Bourguignon MH, Benvenuti C, Duval AM, Agostini D, Loisance D, Castaigne A, Syrota A. Prognostic value of cardiac metaiodobenzylguanidine in patients with heart failure. J Nucl Med 1992;33:471-7.
36. Nakata T, Miyamoto K, Doi A, Sasso H, Wakabayashi T, Kobayashi H, Tsuchihashi K, Shimamoto K. Cardiac death prediction and impaired cardiac sympathetic innervation assessed by MIBG in patients with failing and nonfailing hearts. J Nucl Cardiol 1998;5:579-90.
37. Wakabayashi T, Nakata T, Hashimoto A, Yuda S, Tsuchihashi K, Travin MI, Shimamoto K. Assessment of underlying etiology and cardiac sympathetic innervation to identify patients at high risk of cardiac death. J Nucl Med 2001;42:1757-67.
38. Kioka H, Yamada T, Mine T, Morita T, Tsukamoto Y, Tamaki S, Masuda M, Okuda K, Hori M, Fukunami M. Prediction of sudden death in patients with mild-to-moderate chronic heart failure by using cardiac iodine-123 metaiodobenzylguanidine imaging. Heart 2007;93:1213-8.
39. Agostini D, Verberne HJ, Burchert W, Knuuti J, Povince P, Sambuceti G, Unlu M, Estorch M, Banerjee G, Jacobson AF. I-123-*m*IBG myocardial imaging for assessment of risk for a major cardiac event in heart failure patients: Insights from a retrospective European multicenter study. Eur J Nucl Med Mol Imaging 2008;35:535-46.
40. Jacobson AF, Senior R, Cerqueira MD, Wong ND, Thomas GS, Lopez VA, et al. Myocardial iodine-123 meta-iodobenzylguanidine imaging and cardiac events in heart failure: Results of the prospective ADMIRE-HF (AdreView myocardial imaging for risk evaluation in heart failure) study. J Am Coll Cardiol 2010;55. doi: 10.1016/j.jacc.2010.01.014.
41. Travin M, Anathassubramaniam K, Henzlova MJ, Clements IP, Amanullah A, Jacobson AF. Imaging of myocardial sympathetic innervation for prediction of cardiac and all-cause mortality in heart failure: Analysis from the ADMIRE-HF trial. Circulation 2009;120:S350.
42. Lotze U, Kaepplinger S, Kober A, Richartz BM, Gottschild D, Figulla HR. Recovery of the cardiac adrenergic nervous system after long-term β-blocker therapy in idiopathic dilated cardiomyopathy: Assessment by increase in myocardial ^{123}I-metaiodobenzylguanidine uptake. J Nucl Med 2001;42:49-54.
43. Gerson MC, Craft LL, McGuire N, Suresh DP, Abraham WT, Wagoner LE. Carvedilol improves left ventricular function in heart failure patients with idiopathic dilated cardiomyopathy and a wide range of sympathetic nervous system function as measured by iodine 123 metaiodobenzylguanidine. J Nucl Cardiol 2002;9:608-15.
44. Merlet P, Pouillart F, Dubois-Randé J, Delahaye N, Fumey R, Castaigne A, Syrota A. Sympathetic nerve alterations assessed with ^{123}I-MIBG in the failing human heart. J Nucl Med 1999;40:224-31.
45. Cohen-Solal A, Rouzet F, Berdeaux A, Le Guludec D, Abergel E, Syrota A, Merlet P. Effects of carvedilol on myocardial sympathetic innervation in patients with chronic heart failure. J Nucl Med 2005;46:1796-803.
46. Takeishi Y, Atsumi H, Fujiwara S, Takahashi K, Tomoike H. ACE inhibition reduces cardiac iodine-123-MIBG release in heart failure. J Nucl Med 1997;38:1085-9.
47. Toyama T, Aihara Y, Iwasaki T, Hasegawa A, Suzuki T, Nagai R, Endo K, Hoshizaki H, Oshima S, Taniguchi K. Cardiac sympathetic activity estimated by ^{123}I-MIBG myocardial imaging in patients with dilated cardiomyopathy after β-blocker or angiotensin-converting enzyme inhibitor therapy. J Nucl Med 1999;40:217-23.
48. Kasama S, Toyama T, Kumakura H, Takayama Y, Ichikawa S, Suzuki T, Kurabayashi M. Spironolactone improves cardiac sympathetic nerve activity and symptoms in patients with congestive heart failure. J Nucl Med 2002;43:1279-85.
49. Kasama S, Toyama T, Kumakura H, Takayama Y, Ichikawa S, Suzuki T, Kurabayashi M. Addition of valsartan to an angiotensin-converting enzyme inhibitor improves cardiac sympathetic nerve activity and left ventricular function in patients with congestive heart failure. J Nucl Med 2003;44:884-90.
50. Toyama T, Hoshizaki H, Seki R, Isobe N, Adachi H, Naito S, Oshima S, Taniguchi K. Efficacy of amiodarone treatment on cardiac symptom, function, and sympathetic nerve activity in patients with dilated cardiomyopathy: Comparison with β-blocker therapy. J Nucl Cardiol 2004;11:134-41.
51. Suwa M, Otake Y, Moriguchi A, Ito T, Hirota Y, Kawamura K, Adachi I, Narabayashi I. Iodine-123 metaiodobenzylguanidine myocardial scintigraphy for prediction of response to β-blocker therapy in patients with dilated cardiomyopathy. Am Heart J 1997;133:353-8.
52. Choi JY, Lee KH, Hong KP, Kim BT, Seo JD, Lee WR, Lee SH. Iodine-123 MIBG imaging before treatment of heart failure with carvedilol to predict improvement of left ventricular function and exercise capacity. J Nucl Cardiol 2001;8:4-9.
53. Udelson JE, Shafer CD, Carrió I. Radionuclide imaging in heart failure: Assessing etiology and outcomes and implications for management. J Nucl Cardiol 2002;9:S40-52.
54. Matsui T, Tsutamoto T, Maeda K, Kusukawa J, Kinoshita M. Prognostic value of repeated 123I-metaiodobenzylguanidine imaging in patients with dilated cardiomyopathy with congestive heart failure before and after optimized treatments—comparison with neurohumoral factors. Circ J 2002;66:537-43.
55. Drakos SG, Athanasoulis T, Malliaras KG, Terrovitis JV, Diakos N, Koudoumas D, Ntalianis AS, Theodoropoulos SP, Yacoub MH, Nanas JN. Myocardial sympathetic innervation and long-term left ventricular mechanical unloading. J Am Coll Cardiol Img 2010;3:64-70.
56. D'Orio Nishioka SA, Filho MM, Soares Brandão SC, Clementina Giorgi M, Vieira MLC, Costa R, Mathias W, Cláudio Meneghetti J. Cardiac sympathetic activity pre and post resynchronization therapy evaluated by ^{123}I-MIBG myocardial scintigraphy. J Nucl Cardiol 2007;14:852-9.
57. Tomaselli GF, Zipes DP. What causes sudden death in heart failure? Circ Res 2004;95:754-63.
58. Bardy GH, Lee KL, Mark DB, et al. Amiodarone or an implantable defibrillator for congestive heart failure. N Engl J Med 2005;352:225-37.
59. Jessup M, Abraham WT, Casey DE, Feldman AM, Francis GS, Ganiats TG, Konstam MA, Mancini DM, Rahko PS, Silver MA, Stevenson LW, Yancy CW. Writing on behalf of the 2005 Guideline Update for the Diagnosis and Management of Chronic Heart Failure ion the Adult Writing Committee. 2009 focused update: ACCF/AHA guidelines for the diagnosis and management of heart failure in adults: A report of the American College of Cardiology/American heart Association Task Force on Practice Guidelines. J Am Coll Cardiol 2009;53:1343-82.
60. Fisher JD, Hector HE. Relative and absolute benefits: Main results should be reported in absolute terms. PACE 2007;30:935-7.
61. Passman R, Kadish A. Sudden death prevention with implantable devices. Circulation 2007;116:561-71.
62. Desai A, Fang J, Maisel W, Baughman K. Implantable defibrillators for the prevention of mortality in patients with nonischemic cardiomyopathy: A meta-analysis of randomized controlled rates. JAMA 2004;292:2874-9.

63. Buxton AE, Lee KL, Hafley GE, Pires LA, Fisher JD, Gold MR, Josephson ME, Lehmann MH. Limitations of ejection fraction for prediction of sudden death risk in patients with coronary artery disease. J Am Coll Cardiol 2007;50:1150-7.
64. Goldenberg I, Vyas AK, Hall WJ, Moss AJ, Wang H, He H, Zareba W, McNitt S, Andrews ML. Risk stratification for primary implantation of a cardioverter-defibrillator in patients with ischemic left ventricular dysfunction. J Am Coll Cardiol 2008;51: 288-96.
65. Passman R, Kadish A. Shouldn't everyone have an implantable cardioverter-defibrillator? Circulation 2009;120:2166-7.
66. Sanders GD, Hlatky MA, Owens DK. Cost-effectiveness of implantable cardioverter-defibrillators. N Engl J Med 2005;353: 1471-80.
67. Barron HV, Lesh MD. Autonomic nervous system and sudden cardiac death. J Am Coll Cardiol 1996;27:1053-60.
68. Stanton MS, Tuli MM, Radtke NL, Heger JJ, Miles WM, Mock BH, Burt RW, Wellman HN, Zipes DP. Regional sympathetic denervation after MI in humans detected noninvasively using I-123-MIBG. J Am Coll Cardiol 1989;14:1519-26.
69. McGhie AI, Corbett JR, Akers MS, Kulkarni P, Sills MN, Kremers M, Buja M, Durant-Reville M, Parkey RW, Willerson JT. Regional cardiac adrenergic function using I-123 MIBG SPECT imaging after acute myocardial infarction. Am J Cardiol 1991;67: 236-42.
70. Arora R, Ferrick KJ, Nakata T, Kaplan RC, Rozengarten M, Latif F, Ng K, Marcano V, Heller S, Fisher JD, Travin MI. I-123 MIBG imaging and heart rate variability analysis to predict the need for an implantable cardioverter defibrillator. J Nucl Cardiol 2003;10: 121-31.
71. Nagahara D, Nakata T, Hashimoto A, Wakabayashi T, Kyuma M, Noda R, Shimoshige S, Uno K, Tsuchihashi K, Shimamoto K. Predicting the need for an implantable cardioverter defibrillator using cardiac metaiodobenzylguanidine activity together with plasma natriuretic peptide concentration or left ventricular function. J Nucl Med 2008;49:225-33.
72. Senior R, Agostini D, Travin M, Caldwell J, Gerson MC, Jacobson AF. Imaging of myocardial sympathetic innervation for prediction of arrhythmic events in heart failure patients: Insights from the ADMIRE-HF trial. Circulation 2009;120:S349.
73. Boogers MM, Willem CJ, Henneman MM, Van Bommel RJ, Boersma E, Dibbets-Schneider P, et al. Cardiac sympathetic denervation assessed with 123-Iodine Metaiodobenzylguanidine imaging predicts ventricular arrhythmias in patients with implantable cardioverter-defibrillator. Circulation 2009;120: S348-9.
74. Tamaki S, Yamada T, Okuyama Y, Morita T, Sanada S, Tsukamoto Y, et al. Cardiac iodine-123 metaiodobenzylguanidine imaging predicts sudden cardiac death independently of left ventricular ejection fraction in patients with chronic heart failure and left ventricular systolic dysfunction: Results from a comparative study with signal-averaged electrocardiogram, heart rate variability, and QT dispersion. J Am Coll Cardiol 2009;53:426-35.
75. Mitrani RD, Klein LS, Miles WM, Hackett FK, Burt RW, Wellman HN, Zipes DP. Regional cardiac sympathetic denervation in patients with ventricular tachycardia in the absence of coronary artery disease. J Am Coll Cardiol 1993;22:1344-53.
76. Gill JS, Hunter GJ, Gane J, Ward DE, Camm AJ. Asymmetry of cardiac [^{123}I] meta-iodobenzylguanidine scans in patients with ventricular tachycardia and a ''clinically normal'' heart. Br Heart J 1993;69:6-13.
77. Schäfers M, Lerch H, Wichter T, Rhodes CG, Lammertsma AA, Borggrefe M, Hermansen F, Schober O, Breithardt G, Camici PG. Cardiac sympathetic innervation in patients with idiopathic right ventricular outflow tract tachycardia. J Am Coll Cardiol 1198;32: 181-6.
78. Wichter T, Matheja P, Eckardt L, Kies P, Schäfers K, Schulze-Bahr E, Haverkamp W, Borggrefe M, Schober O, Breithardt G, Schäfers M. Cardiac autonomic dysfunction in Brugada syndrome. Circulation 2002;105:702-6.
79. Wilson RF, Christensen BV, Olivari MT, Simon Am White CW, Laxson DD. Evidence for structural sympathetic reinnervation after orthotopic cardiac transplantation in humans. Circulation 1991;38:1210-20.
80. Hunt S. Reinnervation of the transplanted heart—why is it important? N Engl J Med 2001;345:762-4.
81. Schwaiger M, Hutchins GD, Kalff V, Rosenspire K, Haka MS, Mallette S, Deeb GM, Abrams GD, Wieland D. Evidence for regional catecholamine uptake and storage sites in the transplanted human heart by positron emission tomography. J Clin Invest 1991;87:1681-90.
82. Bengel FM, Ueberfuhr P, Ziegler SI, Nekolla S, Reichart B, Schwaiger M. Serial assessment of sympathetic reinnervation after orthotopic heart transplantation. A longitudinal study using PET and C-11 hydroxyephedrine. Circulation 1999;99:1866-71.
83. Bengel FM, Ueberfuhr P, Schiepel N, Nekolla SG, Reichart B, Schwaiger M. Effect of sympathetic reinnervation on cardiac performance after heart transplantation. N Engl J Med 2001;345: 731-8.
84. Watanabe K, Takahashi T, Miyajima S, Hirokawa Y, Tanabe N, Kato K, Kodama M, Aizawa Y, Tazawa S, Inoue M. Myocardial sympathetic denervation, fatty acid metabolism, and left ventricular wall motion in vasospastic angina. J Nucl Med 2002;43: 1476-81.
85. Tomoda H, Yoshioka K, Shiina Y, Tagawa R, Ide M, Suzuki Y. Regional sympathetic denervation detected by iodine 123 metaiodobenzylguanidine in non-Q-wave myocardial infarction and unstable angina. Am Heart J 1994;128:452-8.
86. Stevens MJ, Raffel DM, Allman KC, Dayanikli F, Ficaro E, Sandford T, Wieland DM, Pfeifer MA, Schwaiger M. Cardiac sympathetic dysinnervationin diabetes. Implications for enhanced cardiovascular risk. Circulation 1998;98:961-8.
87. Nagamachi S, Fujita S, Nishii R, Futami S, Tamura S, Mizuta M, Nakazato M, Kurose T, Wakamatsu H. Prognostic value of cardiac I-123 metaiodobenzylguanidine imaging in patients with non-insulin-dependent diabetes mellitus. J Nucl Cardiol 2006;13: 34-42.
88. Wakasugi S, Fischman AJ, Babich JW, Aretz HT, Callahan RJ, Nakaki M, Wilkinson R, Strauss HW. Metaiodobenzylguanidine: Evaluation of its potential as a tracer for monitoring doxorubicin cardiomyopathy. J Nucl Med 1993;34:1282-6.
89. Olmos RA, ten Bokkel Huinink WW, ten Hoeve RFA, Van Tinteren H, Bruning PF, Van Vlies B, Hoefnagel CA. Adrenergic derangement by [^{123}I]Metaiodobenzylguanidine scintigraphy. Eur J Cancer 1995;31A:26-31.
90. Carrió I, Estorch M, Berná L, López-Pousa J, Tabernero J, Torres G. Indium-111-antimyosin and iodine-123-MIBG studies in early assessment of doxorubicin cardiotoxicity. J Nucl Med 1995;36: 2024-49.
91. Lautamäki R, Tipre D, Bengel FM. Cardiac sympathetic neuronal imaging using PET. Eur J Nucl Med Mol Imaging 2007;34: S74-85.
92. Caldwell JH, Link JM, Levy WC, Poole JE, Stratton JR. Evidence for pre- to postsynaptic mismatch of the cardiac sympathetic nervous system in ischemic congestive heart failure. J Nucl Med 2008;49:234-41.
93. Arora R, Ng J, Ulphani J, Mylonas I, Subacius H, Shade G, Gordon D, Morris A, He X, Lu Y, Belin R, Goldberger JJ, Kadish

AH. Unique autonomic profile of the pulmonary veins and posterior left atrium. J Am Coll Cardiol 2007;49:1340-8.
94. Lellouche N, Buch E, Celigoj A, Siegerman C, Cesario D, De Diego C, Mahajan A, Boyle NG, Wiener I, Garfinkel A, Shivkumar K. Functional characterization of atrial electrograms in sinus rhythm delineates sites of parasympathetic innervation in patients with paroxysmal atrial fibrillation. J Am Coll Cardiol 2007;50:1324-31.